Numerical study of the exchange bias effects in magnetic nanoparticles with core/shell morphology

E. Eftaxias* and K. N. Trohidou
Institute of Materials Science, NCSR Demokritos, 15310 Athens, Greece
(Received 3 September 2004; published 11 April 2005)

We have used the Monte Carlo simulation technique to investigate the effect of an antiferromagnetic shell on the exchange bias and the coercive fields of composite magnetic nanoparticles with core/shell morphology. We find that the exchange bias field depends mainly on the structure of the interface and less on its size, while the coercive field depends mainly on the interface size. A reduction of the core thickness for a given particle size results in an increase of both exchange bias and coercive fields. An increase of the shell thickness for a given core size enhances the exchange bias field and reduces the coercive field. An increase in the strength of the interface and shell-exchange coupling constant results in an increase of the exchange bias field and a reduction of the coercive field. In all cases the exchange bias field has a stronger temperature dependence than the coercive field. Our results are in good agreement with experimental findings.

DOI: 10.1103/PhysRevB.71.134406 PACS number(s): 75.50.Tt, 75.50.Vv, 75.50.Ss, 75.40.Mg

I. INTRODUCTION

The requirement to increase the recording density in magnetic recording media leads to the reduction of the grain size of magnetic nanoparticles. A limitation of this reduction is the instability of the ferromagnetic behavior of the nanoparticles because of thermal fluctuations. The requirement to keep the magnetic behavior of the nanoparticles stable at room temperature can be achieved by enhancement of the magnetic anisotropy. In view of this, many experiments have been concentrated recently on the effect of the surface oxidation on the magnetic properties of ferromagnetic (FM) nanoparticles. In samples where the ferromagnetic core diameters were smaller than 10 nm,[1–3] enhanced coercivities were measured after the oxidation, whereas in samples with core diameters of the order of 50 nm, the coercive fields measured before and after the oxidation were not very different.[4]

In nanoparticles with an Fe core[5] surrounded by an Fe-oxide shell, high coercivity values were observed at low temperatures with drastic temperature dependence.[5] The highest coercivity obtained in Ref. 5 at room temperature was 1050 Oe for a particle with a 14 nm core diameter, and its value at 10 K was 1425 Oe, whereas in a sample with a core diameter of 2.5 nm the coercivity decreased from a value of 3400 Oe at 10 K to a negligible value at 150 K. Thus, in smaller particles the temperature dependence of the coercivity is much stronger than in bigger particles. In smaller particles the Fe core feels much more the effect of the Fe-oxide shell, due to a higher Fe-oxide to Fe ratio. The strong decrease of coercivity with temperature was explained by the superparamagnetic behavior of the Fe-oxide shell and its low blocking temperature. It is estimated that the Fe-oxide shell becomes superparamagnetic at $T \sim 10$–50 K.[1,2] In all experiments on oxide-coated particles, shifted hysteresis loops have been obtained at low temperatures. In nanoparticles with an Fe core of radius 6–7 nm embedded in a Cr_2O_3 matrix the temperature below which the loops are asymmetric is close to 300 K,[6] but it is much lower (close to 120 K) when they are covered by a shell with Fe_2O_3 and Fe_3O_4.[7–10] Moreover, in Co nanoparticles covered by a CoO shell this temperature is below 200 K (Refs. 11 and 12) and in Co/MnO (Ref. 13) thin films it is between 90 and 200 K, depending on the oxygen content. The loops always become symmetric at temperatures above the Néel temperature of the oxide. The shifted hysteresis loop has been attributed to the exchange interaction between the ferromagnetic core and the oxide shell that induces an anisotropy known as exchange anisotropy, and it is unidirectional.[14]

The discovery of the exchange anisotropy on Co/CoO nanoparticles[14] was followed by extensive studies of its effect on several systems and mainly on layered systems[15] with a ferromagnetic/antiferromagnetic (FM/AFM) interface. Up to now several models have been developed to explain the exchange anisotropy in layered structures. In the approach introduced by Malozemoff[16] there is no exchange bias field in the perfect FM/AFM interface of a spin valve; the existence of the exchange bias field is attributed to the interface's roughness. According to the model developed by Schulthess and Butler[17] the exchange bias field is attributed to additional mechanisms such as uncompensated spins at the interface of the antiferromagnet. Nowak and his collaborators[18] demonstrated that the exchange bias field is due to magnetic domains, which are created in a diluted antiferromagnet. Though these models try to explain the effect of the exchange anisotropy in spin valves, we expect that the same physical arguments will be held for the nanoparticles. The fact that the spins of the AFM shell which are coupled to the spins of the ferromagnetic core are not equally distributed on the FM/AFM interface of the nanoparticle makes the interface imperfect even in the absence of additional roughness[16] or lattice vacancies.[18]

In our previous study on composite FM/AFM nanoparticles[19] we have demonstrated that the existence of the AFM shell itself induces the exchange anisotropy along the interface that is in turn responsible for the fact that the smaller nanoparticles have higher coercive fields than the bigger ones at low temperatures. In this work using the

Monte Carlo (MC) simulation technique we perform a systematic study of the exchange bias effects of composite FM/AFM to reveal the factors that influence the size and the temperature dependence of the shifted hysteresis loops.

In the experimental situation there are several cases in which the ferromagnetic core is surrounded by a ferrimagnetic oxide.[7] In the present work only the case of an antiferromagnetic shell is considered. There is experimental evidence that the effect of the exchange anisotropy is more pronounced in this case.[14,15,20]

The remainder of the paper is organized as follows. In Sec. II, we describe the model of the magnetic structure of the nanoparticles and the method of calculation of the exchange bias field. In Sec. III we present numerical results and discuss the dependence of the exchange bias and the coercive fields on the interface structure, the shell thickness, and the strength of the interface and the shell exchange coupling constant. A discussion of our results is given in Sec. IV.

II. THE MODEL

We consider spherical nanoparticles of radii R, expressed in lattice spacings, on a simple cubic (sc) lattice. The spins in the particles interact with Heisenberg exchange interaction, and at each crystal site they experience a uniaxial anisotropy. At the surface of the particles, the crystal symmetry is reduced and consequently the anisotropy is stronger than the bulk.[21] The same argument holds obviously for the interface of the composite particles. The antiferromagnetic shell is considered as a layer surrounding the core.

In the presence of an external magnetic field, the energy of the system is

$$H = -J_{\mathrm{FM}} \sum_{\langle i,j \in \mathrm{FM} \rangle} \vec{S}_i \cdot \vec{S}_j - \sum_{i \in \mathrm{FM}} K_{i\mathrm{FM}} (\vec{S}_i \cdot \hat{e}_i)^2 - J_{\mathrm{AF}} \sum_{\langle i,j \in \mathrm{AF} \rangle} \vec{S}_i \cdot \vec{S}_j - \sum_{i \in \mathrm{AF}} K_{i\mathrm{AF}} (\vec{S}_i \cdot \hat{e}_i)^2 - J_{\mathrm{IF}} \sum_{\langle i \in \mathrm{FM}, j \in \mathrm{AF} \rangle} \vec{S}_i \cdot \vec{S}_j - \vec{H} \cdot \sum_i \vec{S}_i .$$

Here S_i is the atomic spin at site i and $\hat{e}_i$ is the unit vector in the direction of the easy axis at site i. The angular brackets in the sums denote a summation over the nearest neighbors only. The first term gives the exchange interaction between the spins in the ferromagnetic core (the exchange coupling constant J_{FM}, which is taken as equal to one). The second term gives the anisotropy energy of the ferromagnetic core. If the site i lies in the outer layer of the ferromagnetic core $K_{i\mathrm{FM}}=K_{\mathrm{IF}}$, and $K_{i\mathrm{FM}}=K_C$ elsewhere. The third term gives the exchange interaction in the antiferromagnetic shell (the exchange coupling constant J_{AF}), and the fourth term gives the anisotropy energy of the antiferromagnetic shell. The fifth term gives the exchange interaction at the interface between the core and the shell (the exchange coupling constant J_{IF}), and the last term is the energy in the presence of an external magnetic field. We set $J_{\mathrm{AF}}=J_{\mathrm{FM}}/2$, because the Neél temperature of the antiferromagnetic oxide is lower than the Curie temperature of the corresponding ferromagnet. The interface-exchange coupling constant J_{IF} is equal to the J_{AF} in size, in agreement with theoretical studies in layered systems[17,18,22] ($J_{\mathrm{IF}}=J_{\mathrm{FM}}/2$), and the interaction is considered ferromagnetic. If i lies in the outer layer of the antiferromagnetic shell then $K_{i\mathrm{AF}}=K_S$ and $K_{i\mathrm{AF}}=K_{\mathrm{SH}}$ inside the shell. We take the anisotropy along the z axis in the core, at the interface, and in the shell. At the surface of the nanoparticles the anisotropy is taken random.[23]

The Monte Carlo simulations are performed using the Metropolis algorithm. We use from 18 000 up to 40 000 Monte Carlo steps per spin,[24] depending on the system size. Our results are checked by repeating the runs for a sequence of ten random numbers. The statistical error is negligible, so it does not appear in our plots.

The coercive field H_c is defined as the magnetic field that reverses the magnetization of the particle in the simulation time, so that the z component of the magnetization vanishes. The exchange bias field H_{ex}, induced by the exchange anisotropy, is defined as the mean difference of the fields that vanish the z component of the magnetization in the two branches of the hysteresis loops. H, H_c , and H_{ex} are given in units of $J_{\mathrm{FM}}/g\mu_B$, T in units of J_{FM}/k, and the anisotropy coupling constants in units of J_{FM}. For the sc lattice, $T_c=2.9$ and $T_N=1.5$.[25]

In the experiments, the observed coercive loops of these particles after the field-cooling procedure are shifted.[14,15] We simulate the field-cooling procedure starting with an unmagnetized nanoparticle at temperature $T=2.5$ (which is between the T_c of the ferromagnetic core and the Neél temperature of the antiferromagnetic shell), and consequently we cool the nanoparticle in the presence of a magnetic field h_L along the z axis.

III. RESULTS AND DISCUSSION

We present in this section our results on spherical magnetic nanoparticles with core/shell morphology using the MC simulation technique, in which the microstructure and the temperature are explicitly included. The parameters used in the model are the particle size R expressed in lattice spacings, the three exchange coupling constants J, and the four anisotropy coupling constants K, for different parts of the particle. Our results are presented for a set of these parameters in order to discuss the physics emerging from some morphology characteristics of these systems. We start with a shell thickness equal to four lattice spacings; the surface thickness is one lattice spacing. The values we use for the anisotropy coupling constants are $K_C=0.05, K_{\mathrm{IF}}=0.5, K_{\mathrm{SH}}=0.5$, and $K_S=1.0$. The cooling field is taken as $h_L=0.7$ in our units.

If we assume that the exchange interaction along the interface is ferromagnetic the bond energy for the spins across the FM/AFM interface is minimum when they are aligned as parallel and maximum when they aligned as antiparallel. The opposite would happen in the case of an AFM interaction along the interface. During the field-cooling procedure the spins are aligned in such a way that the energy of the system is minimum. Along these lines, for an FM interface interaction the parallel spin alignment is favorable. This alignment together with the strong interface anisotropy makes it hard

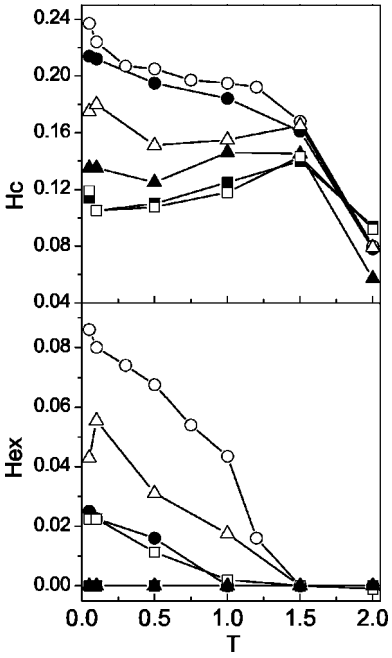

FIG. 1. Coercive field and exchange bias field versus temperature for three sets of particles with similar sizes but very different proportions of up bonds at the interface $R=10$ (closed circles) and $R=11.0$ (open circles), $R=12.0$ (closed triangles) and $R=12.35$ (open triangles), and $R=17.0$ (closed squares) and $R=19.0$ (open squares).

for the spins to turn when the field goes from h to $-h$, and it results in a high coercive field. When the spins align along the negative direction, by changing the field again from $-h$ to h they need less energy to turn. Developing this picture we will call up bonds the pairs of spins along the FM/AFM interface which are parallel and down bonds the antiparallel ones. So a nanoparticle with a radius of $R=10.0$ has up bonds=360 and down bonds=318, and the nanoparticle with a radius of $R=11.0$ has up bonds=606 and down bonds=288. We can see that though these two particles are very close in size they have very different numbers of up and down bonds. The same holds for the nanoparticles with sizes 17.0 and 19.0. They have $R=17.0$ (up bonds=1590, down bonds =1584) and $R=19.0$ (up bonds=2502, down bonds=1752). The effect is more pronounced in the case of radii of $R=12.0$ (up bonds=552, down bonds=630) and $R=12.35$ (up bonds=840, down bonds=486). Though these nanoparticles are very similar in size the proportion of up bonds is 46.7% and 63.3%, respectively.

Our results for the coercive field and the exchange bias field as a function of temperature are shown in Fig. 1 for the pairs of particles with radii of 10.0 and 11.0 (circles), 12.0 and 12.35 (triangles), and 17.0 and 19.0 (squares). What we observe in Fig. 1 for the coercive field is the following: if we compare each pair of particles of similar size, the ones with a bigger proportion of up bonds have higher coercive fields. The difference is more pronounced in the pair of particles with sizes 12.0 and 12.35. They have the biggest difference in the proportion of up bonds. As the temperature increases the thermal fluctuations cancel the interface effects. If we now compare the pair of particles, the size dependence of the coercive field as a function of temperature has no difference in behavior from the one observed previously.[19] The smaller particles have a higher coercive field at low temperatures than the bigger ones, and this behavior is reversed at higher temperatures.

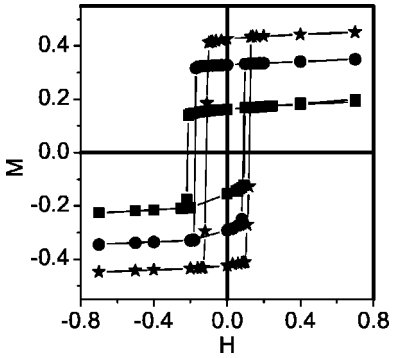

FIG. 2. Hysteresis loops for particles with radii of $R=9.0$ (squares), $R=12.35$ (circles), and $R=16.0$ (stars) at $T=0.05$ and a shell thickness of 4 lattice spacings.

In the exchange bias field curves, however, we observe that the size dependence on the number of bonds and not so much on the actual size of the particle plays on important role in the temperature dependence of the exchange bias field. When the difference of the up and down bonds is big, such as the $R=11.0$, 12.35, and 19.0 cases, the particle magnetization turns easily by going from the $-h$ to the h field. The exchange bias field is stronger, and it follows the temperature dependence of the coercive field, while in the case of small up or down bonds, the difference in the behavior of the two branches of the hysteresis loop is similar. This results in a reduced exchange bias field with a strong temperature dependence. The temperature dependence of the exchange field is in good agreement with the experimental findings of Ref. 13.

Next, we study the influence of the shell thickness on the behavior of the hysteresis loop and the thermal dependence of the coercive and exchange bias fields. We consider three particles with radii of $R=9.0$ ($N=3071$, $N_{\mathrm{FM}}=515$, $N_{\mathrm{AFM}}=2556$), $R=12.35$ ($N=7881$, $N_{\mathrm{FM}}=2469$, $N_{\mathrm{AF}}=5412$), and $R=16.0$ ($N=17077$, $N_{\mathrm{FM}}=7153$, $N_{\mathrm{AF}}=9924$) an AFM shell of 4 lattice spacings thick and particles with the same total radii but antiferromagnetic shells of 6 lattice spacings thick, $R=9.0$ ($N=3071$, $N_{\mathrm{FM}}=123$, $N_{\mathrm{AFM}}=2948$), $R=12.35$ ($N=7881$, $N_{\mathrm{FM}}=1045$, $N_{\mathrm{AF}}=6836$), and $R=16.0$ ($N=17077$, $N_{\mathrm{FM}}=4169$, $N_{\mathrm{AF}}=12908$). Here N, N_{FM}, and N_{AFM} are the total number of spins, the number of the core spins, and the number of the shell spins in the nanoparticles, respectively. In the former case the inner part of the shell is considered 3 lattice spacings thick and in the latter 5 lattice spacings thick. The surface thickness is 1 lattice spacing in both cases. The results for the hysteresis loops for these three particles are shown in Figs. 2 and 3 at a very low temperature $T=0.05$, for shell thicknesses 4 and 6 lattice spacings, respectively. As we can see, the hysteresis loops are shifted. Also it appears that the smaller particles have the bigger shifting and the bigger coercive field. This is in agreement with the experimental findings.[7,11,26] In Fig. 4 we show

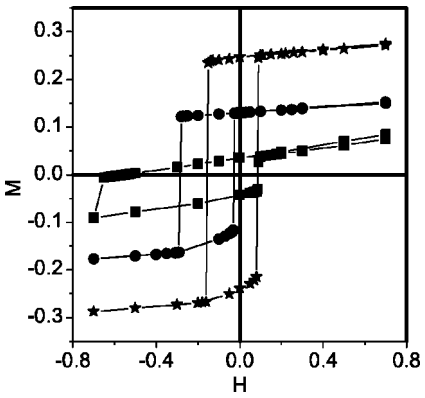

FIG. 3. Hysteresis loops for particles with radii $R=9.0$ (squares), $R=12.35$ (circles), and $R=16.0$ (stars) at $T=0.05$ and a shell thickness of 6 lattice spacings.

the coercive and exchange bias fields as a function of temperature. We can see that for the thickness of 4 lattice spacings (solid lines) at low temperatures there is a size reversal to the temperature dependence of the coercive and exchange bias fields. In the second case we consider a shell of 6 lattice spacings thick with the other parameters being the same as those we show in Fig. 3. The hysteresis loops for the nanoparticles are of the same size as previously, but in this case the core and shell thickness have changed. We observe in this case the same size dependence of the coercive field, but an increase in size of both the coercive and exchange bias fields. This increase is also shown in the temperature dependence of these quantities in Fig. 4 (broken lines and open symbols). This behavior is in agreement with experimental results[27] on

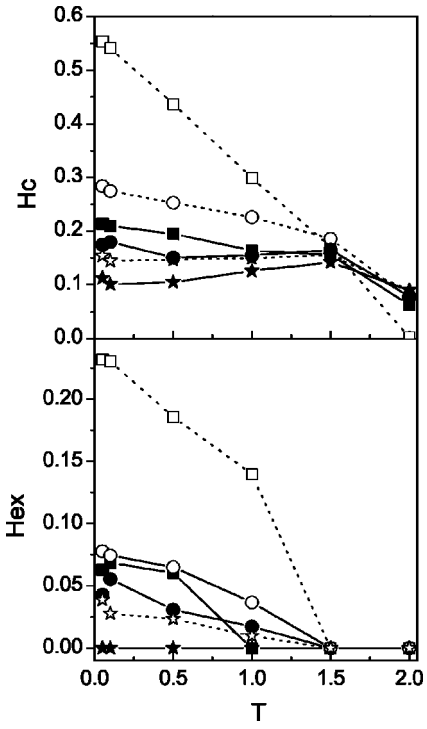

FIG. 4. Coercive field and exchange bias field vs temperature for particles with radii of $R=9.0$ (squares), $R=12.35$ (circles), and $R=16.0$ (stars), and a shell thickness, of 4 lattice spacings (closed symbols) and 6 lattice spacings (open symbols).

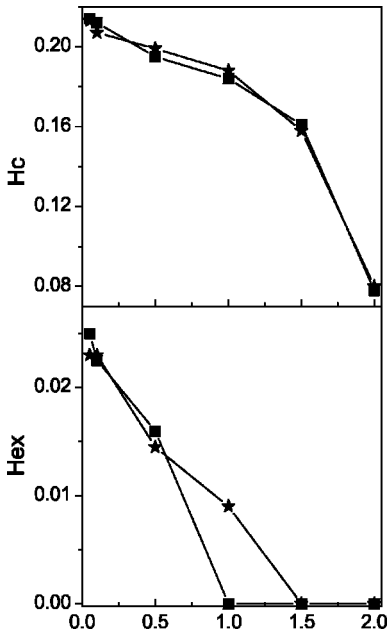

FIG. 5. Coercive field and exchange bias field vs temperature for two particles with the same ferromagnetic radii of $R_{FM}=6.0$ lattice spacings and a shell thickness of 4 lattice spacings [total radius of $R=10.0$ (squares)] and 6 lattice spacings [total radius of $R=12.0$ (stars)].

Co/CoO nanoparticles, in which the authors they observe an increase in size with an increasing oxygen dose. These results demonstrate once more the important role of the interface, because they show that the particles with the smaller ferromagnetic radii, i.e., bigger interface contributions, have stronger coercive and exchange bias fields.

To further demonstrate the role of the interface and the shell thickness, we keep the core thickness constant and we increase the shell thickness. In Fig. 5, we plot the coercive and the exchange bias fields versus temperature, respectively, for two particles of sizes $R=10.0$ and $R=12.0$, with the same core thickness equal to 6 lattice spacings and shell thicknesses of 4 and 6 lattice spacings, respectively. We observe that the results are the same for both particles at all temperatures for the coercive field. The exchange bias field is the same for both particles at low temperatures, but as the temperature increases the one with the biggest shell thickness has higher values for the H_{ex}. The exchange bias field is due entirely to the existence of the FM/AFM interface of the core/shell nanoparticle. Consequently the influence of the thermal fluctuations on the interface will depend on the shell thickness.

For a further study of the effect of the shell thickness on the exchange bias field we consider a ferromagnetic particle with core radii of 7 lattice spacings and anisotropy coupling constants of $K_c=0.05$ and $K_{IF}=0.5$, and we start to add AF layers with uniaxial anisotropy along the z axis and anisotropy constant $K_{SH}=0.5$. As it can be seen from Fig. 6 where we plot the exchange bias field as a function of the shell thickness for two temperatures, at the low temperature this field is approximately constant after the second layer. This result is in agreement with the experimental findings of Ref. 27, in which they observe very fast stabilization of the ex-

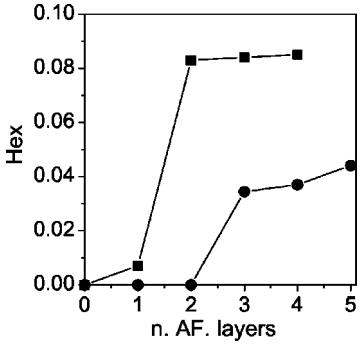

FIG. 6. Exchange bias field as a function of the shell thickness, starting from a particle with a ferromagnetic radii of $R_{FM}=7.0$, at two temperatures $T=0.05$ (squares) and $T=1.0$ (circles).

change bias field with the oxygen dose in Co/CoO nanoparticles. However, with the increase in the temperature to $T=1.0$ in our units, more AF layers are needed to increase and stabilize the exchange bias field. These results show that because of the thermal fluctuations at the interface configuration we need a thicker shell to stabilize the interface contribution.

Finally, we examine the effect of the strength of the interface-exchange coupling and the antiferromagnetic exchange coupling constant, keeping the shell thickness of 4 lattice spacings and the other parameters as they were previously. We first increase the interface coupling constant J_{IF}, taking it now as equal to J_{FM}. The results for the temperature dependence of the coercive and the exchange bias fields for a particle with size $R=11.0$ are shown in Fig. 7 (circles). In the same figure the results for $J_{IF}=J_{FM}/2$ (triangles) are shown for comparison. From this figure we can see that an increase in the strength of the interface-exchange coupling results in a reduction of the coercive field at low temperatures and an enhancement of the exchange bias field. This is due to the fact that the stronger interface-exchange coupling results in a faster reversal of the ferromagnetically aligned spins with the antiferromagnetic shell. At temperatures higher than T_{Neel} the behavior is similar to that of $J_{IF}=J_{FM}/2$, because at these temperatures the shell becomes paramagnetic and does not influence the ferromagnetic core.

Keeping the interface-exchange coupling constant enhanced as previously and increasing also the exchange coupling constant for the AF shell, we take $J_{AF}=J_{FM}$, and we calculate the exchange bias and the coercive fields for $R=11.0$ as functions of temperature. In this case the $T_{\text{Néel}}$ and T_{Curie} are identical. Results are also shown in Fig. 7 (squares). The increase in the antiferromagnetic exchange coupling constant strength results in a reduction of the coercivity. The exchange bias field is increased and also persists at high temperatures as expected because now $T_{\text{Néel}}$ is higher than it was in the previous cases.

We note here that taking the surface anisotropy radial[28,29] in our simulations has a minor effect on our results. This is expected because, as we showed above in the composite nanoparticles, the major contribution to the exchange bias effects comes from the interface and the first surface layers.

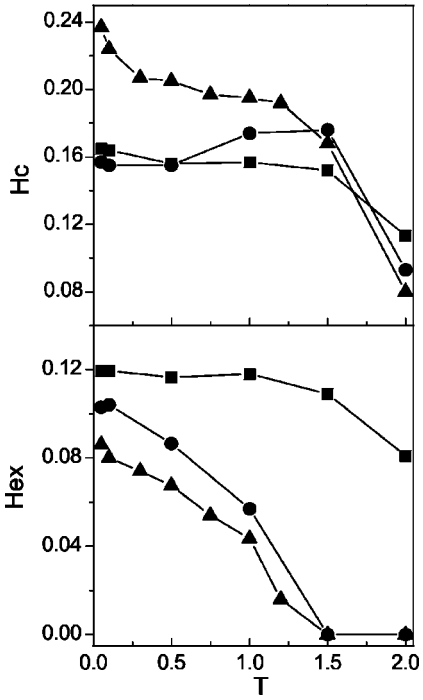

FIG. 7. Coercive field and exchange bias field vs temperature for a particle with a radius of $R=11.0$ with (a) $J_{IF}=0.5$ and $J_{AFM}=0.5$ (triangles), (b) $J_{IF}=1.0$ and $J_{AFM}=0.5$ (circles), and (c) $J_{IF}=1.0$ and $J_{AFM}=1.0$ (squares).

IV. CONCLUSIONS

We have presented a systematic study of the coercive behavior of composite nanoparticles with core/shell morphology, consisting of ferromagnetic and antiferromagnetic shells. We assumed a Heisenberg exchange interaction between the spins in the ferromagnetic core and the antiferromagnetic shell, and we showed that at low temperatures this interaction together with a strong interface anisotropy results in an exchange bias field and a reversal in the size dependence of coercivity.

The exchange bias field always disappears at temperatures greater than $T_{\text{Néel}}$ of the antiferromagnet in agreement with the experimental findings, and it depends strongly on the specific characteristics of the ferromagnetic or antiferromagnetic interface. We show that the exchange bias field is stronger in the interfaces with a stronger difference between up and down bonds. Generally this difference as a percentage the of total bonds is stronger in smaller nanoparticles and results in more asymmetric hysteresis loops.

The strength of the exchange constant at the FM/AFM interface of the nanoparticles at low temperatures reduces the coercive field and increases the exchange bias field. The increase of both the antiferromagnetic exchange constant and the interface constant causes a reduction in the coercivity, and the exchange bias field persists at higher temperatures.

ACKNOWLEDGMENT

This work has been supported by the IMS Center of Excellence on Nanostructured Materials, Project No. 962, and the British-Greek bilater Collaboration 2003–2005.

*Electronic address: eeftaxias@ims.demokritos.gr

[1] L. Del Bianco, D. Fiorani, A. M. Testa, E. Bonetti, L. Savini, and S. Signiretti, J. Magn. Magn. Mater. **262**, 128 (2003).
[2] X. Lin, A. S. Murthy, G. C. Hadjipanayis, C. Swann, and S. I. Shah, J. Appl. Phys. **76**, 6543 (1994).
[3] S. Yamamuro, K. Sumiyama, T. Kamiyama, and K. Suzuki, J. Appl. Phys. **86**, 5726 (1999).
[4] C. M. Hsu, H. M. Lin, K. R. Tsai, and P. Y. Lee, J. Appl. Phys. **76**, 4793 (1994).
[5] S. Gangopadhyay, G. C. Hadjipanayis, C. M. Sorensen, and K. J. Klabunde, in *Nanophase Materials*, edited by George C. Hadjipanayis and Richard W. Siegel (Kluwer Academic Publishers, Dordrecht, 1994), p. 573.
[6] J. Sort, V. Langlais, S. Doppiu, B. Dieny, S. Surinach, J. S. Munoz, M. D. Baro, Ch. Laurent, and J. Nogues, Nanotechnology **15**, S211 (2004).
[7] L. Del Bianco, D. Fiorani, A. M. Testa, E. Bonetti, L. Savini, and S. Signoretti, Phys. Rev. B **66**, 174418 (2002).
[8] D. L. Peng, T. Hihara, K. Sumiyama, and H. Morikawa, J. Appl. Phys. **92**, 3075 (2002).
[9] L Del Bianco, A. Hernando, M. Multigner, C. Prados, J. C. Sanchez-Lopez, A. Fernadez, C. F. Conde, and A. Conde, J. Appl. Phys. **84**, 2189 (1998).
[10] S. Banerjee, S. Roy, J. W. Chen, and D. Chakravorty, J. Magn. Magn. Mater. **219**, 45 (2000).
[11] D. L. Peng, K. Sumiyama, T. Hihara, S. Yamamuro, and T. J. Konno, Phys. Rev. B **61**, 3103 (2000).
[12] G. H. Wen, R. K. Zheng, K. K. Fung, and X. X. Zhang, J. Magn. Magn. Mater. **270**, 407 (2004).
[13] J. van Lierop, M. A. Schofield, L. H. Lewis, and R. J. Gambino, J. Magn. Magn. Mater. **264**, 146 (2003).
[14] W. H. Meiklejohn and C. P. Bean, Phys. Rev. **105**, 904 (1957).
[15] J. Nogues and Ivan K. Schuller, J. Magn. Magn. Mater. **192**, 203 (1999).
[16] A. P. Malozemoff, Phys. Rev. B **35**, 3679 (1987).
[17] T. C. Schulthess and W. H. Butler, Phys. Rev. Lett. **81**, 4516 (1998).
[18] U. Nowak, K. D. Usadel, J. Keller, P. Miltenyi, B. Beschoten, and G. Guntherodt, Phys. Rev. B **66**, 014430 (2002).
[19] X. Zianni and K. N. Trohidou, J. Phys.: Condens. Matter **10**, 7475 (1998).
[20] A. E. Berkowitz and Kentaro Takano, J. Magn. Magn. Mater. **200**, 552 (1999).
[21] T. Kaneyoshi, J. Phys.: Condens. Matter **3**, 4497 (1991).
[22] Shan-Ho Tsai, D. P. Landau, and Thomas C. Schulthess, J. Appl. Phys. **93**, 8612 (2003).
[23] J. M.D. Coey, Phys. Rev. Lett. **27**, 1140 (1971).
[24] *Applications of Monte Carlo Methods in Statistical Physics*, edited by K. Binder (Springer, Berlin, 1984).
[25] D. W. Wood and N. W. Dalton, Phys. Rev. **159**, 384 (1967).
[26] Carlos Luna, Ma del Puerto Morales, Carlos J Serna, and Manuel Vazquez, Nanotechnology **15**, S293 (2004).
[27] Robert Morel, Ariel Brenac, and Celine Portemont, J. Appl. Phys. **95**, 3757 (2004).
[28] R. H. Kodama and A. E. Berkowitz, Phys. Rev. B **59**, 6321 (1999).
[29] O. Iglesias and A. Labarta, Phys. Rev. B **63**, 184416 (2001).